Published in final edited form as:
J Immunol. 2014 April 1; 192(7): 3011–3020. doi:10.4049/jimmunol.1302003.

Long-term B cell depletion in murine lupus eliminates autoantibody-secreting cells and is associated with alterations in the kidney plasma cell niche[1]

Wensheng Wang[*,‡], **Javier Rangel-Moreno**[*,‡], **Teresa Owen**[*], **Jennifer Barnard**[*], **Sarah Nevarez**[*], **H. Travis Ichikawa**[*,§], and **Jennifer H. Anolik**[*,2]

[*]Department of Medicine, Division of Allergy, Immunology and Rheumatology, University of Rochester Medical Center, Rochester, NY 14642

Abstract

Autoantibodies to double-stranded DNA (dsDNA), produced by auto-reactive plasma cells (PC), are a hallmark of systemic lupus erythematosus (SLE) and play a key role in disease pathogenesis. Recent data suggests that auto-reactive PC accumulate not only in lymphoid tissues but also in the inflamed kidney in lupus nephritis. We hypothesized that the variable efficacy of anti-CD20 (rituximab) mediated B cell depletion (BCD) in SLE may be related to the absence of an effect on auto-reactive PCs in the kidney. Here we report that an enrichment of auto-reactive dsDNA antibody secreting cells (ASC) in the kidney of lupus-prone mice (up to 40% of the ASCs) coincided with a progressive increase in splenic germinal centers (GC) and PCs and an increase in renal expression for PC survival factors (BAFF, APRIL and IL6) and PC attracting chemokines (CXCL12). Short-term treatment with anti-CD20 (4 weeks), neither decreased anti-dsDNA nor IgG ASCs in different anatomical locations. However, long-term treatment (12 weeks) significantly reduced both IgG- and dsDNA specific ASCs. In addition, long-term treatment substantially decreased splenic GC- and PC generation and unexpectedly reduced the expression for PC survival factors in the kidney. These results suggest that prolonged BCD may alter the PC survival niche in the kidney, regulating the accumulation and maintenance of auto-reactive PCs.

INTRODUCTION

Systemic lupus erythematosus (SLE) is prototypic autoimmune disorder characterized by dysregulation in multiple arms of the immune system and the production of hallmark autoantibodies. A central role for B cells in the pathogenesis of this disease has been well established (1–3) and includes both antibody production and antibody-independent mechanisms (4). The latter are highlighted by the abrogation of disease and reduction in activated T cells in B cell deficient lupus-prone mice (2), yet the maintenance of T cell abnormalities in mice with B cells incapable of secreting antibody (5). Autoantibody-independent B cell functions include antigen-presentation, T cell activation and polarization, and dendritic cell (DC) modulation, that are mediated at least in part by the ability of B cells to produce cytokines (6, 7).

[1]This work was supported in part by the Lupus Research Institute. Dr. Anolik's work has been supported by NIH grant R01-AI-077674 and P01-AI078907.

[2]Corresponding author: Jennifer H. Anolik, MD, PhD, Department of Medicine, Division of Allergy, Immunology and Rheumatology, University of Rochester, 601 Elmwood Avenue, Box 695, Rochester, NY 14642. Phone: 585-275-1632; Fax: 585-442-3214, Jennifer_anolik@urmc.rochester.edu.
[‡]These authors contributed equally to the work
[§]Current affiliation Division of Rheumatology, Department of Medicine, Emory University, 255 Whitehead Biomedical Research Building, 615 Michael Street, Atlanta, Georgia 30322

On the other hand, autoantibodies produced by B cells are also critical to disease pathogenesis by both direct and indirect mechanisms. In addition to conventional roles of autoantibodies in SLE via Type II (antibody dependent cytotoxicity) and Type III (immune complex) mechanisms, RNA- and DNA-containing autoantigen-autoantibody complexes can play an active role in propagating the autoimmune process in SLE through Toll-like receptor (TLR) mediated immune cell activation (8–11). Anti-dsDNA antibodies can also directly deposit in the kidney of both SLE patients and lupus mice (12, 13) causing tissue inflammatory damage (14) and leading to end-stage renal disease if untreated.

Thus, decreasing autoantibodies may be critical in the treatment of SLE. B cell depletion (BCD) with rituximab (anti-CD20) has demonstrated efficacy in multiple autoimmune diseases including rheumatoid arthritis, multiple sclerosis, and ANCA associated vasculiltis. However, the precise mechanisms by which depletion of B cells abrogates autoimmunity remain incompletely elucidated. Although several open-label studies of BCD as a targeted treatment have demonstrated clinical benefit in SLE (15–17), only a minority of patients have lasting clinical responses (18, 19). Moreover, the failure of two large randomized trials of BCD in SLE (20) highlights the need to better understand the impact of this therapy on the immune system. In particular, anti-CD20 has variable effects on autoantibodies that are produced by CD20 negative plasma cells.

The variable persistence of autoantibodies after BCD could be explained by the presence of long-lived plasma cells (PCs) and/or the ongoing generation of short-lived plasmablasts. Indeed, both long-lived and short-lived populations of antibody-secreting cells (ASCs) can contribute to chronic humoral autoimmunity in NZB/W mice (21), with up to a surprising 40% of the PCs in the spleen having a half-life of > 6 months. Long-lived PCs have also been well described to home to the bone marrow (BM) (22). Recently, autoantibody secreting PCs were also described as enriched in the kidneys of MRL/lpr (23) and NZB/W (24) lupus prone mice, with a high fraction appearing long-lived based on BrdU labeling (25, 26). Taken together, this suggests that long-lived PCs are a major player in SLE. Whether they are generated in situ in the kidney and/or home to the inflamed tissue and find survival niches is controversial.

In non-autoimmune mouse models, it has been demonstrated that treatment with anti-CD20 antibody depletes mature and memory B cells but has minimal impact on PCs (27, 28). Similarly, we previously found that a short course of B cell depletion in NZB/W mice effectively reduced the progression of nephritis without significant change in autoantibody levels or ASCs in spleen and bone marrow (29). In order to understand the mechanism of action of BCD in lupus, we examined the impact of short-term vs. long-term treatment of lupus-prone NZB/W F1 mice with anti-mouse CD20 antibody (anti-mCD20) on PC generation and maintenance. We show that auto-reactive plasma cells reside in the kidney and are eliminated by prolonged anti-CD20 treatment, with an unexpected reduction in the expression of PC survival factors in the kidney. This is the first demonstration that targeted B cell depletion can alter the survival of auto-reactive PCs in inflammatory sites.

MATERIALS and METHODS

Mice and treatment

Lupus-prone NZB/NZW F1 female mice were purchased from Jackson Laboratories and maintained in a pathogen-free animal facility in the University of Rochester Medical Center. Experiments were performed following the guidelines approved by the University of Rochester Committee on Animal Resources. Different age groups of mice were used to define the kinetics and mechanisms of autoreactive PC generation and maintenance, including 8, 19, and 39 week old mice.

Short-term treatment—NZB/NZW F1 female mice (24–30 wks old) with proteinuria ≥ 2+ (100 mg/dl) received a weekly, retro-orbital injection of 300 μg of anti-mCD20 antibody (IgG2a 18B12, Biogen Idec) (n=6) or control antibody IgG2a (2B8, Biogen Idec) for 4 times and were sacrificed 1 week after the last treatment.

Long-term treatment—27 wks old NZB/NZW F1 female mice (high anti-dsDNA antibody titer: ≥400 unit/ml, negative control: 80 unit/ml) were injected weekly with 300 μg anti-mCD20 antibody or control IgG. One group was treated weekly, 4 times (n=6) and sacrificed 8 wks later. Another group was treated weekly for 12 weeks (n=6) and sacrificed 1 wk after the last treatment. Blood samples were collected for measuring circulating auto-antibodies, and proteinuria was assessed with urine dipstick (Uristix; Bayer) twice per week.

Flow cytometry analysis

Spleen and bone marrow lymphocytes were collected in 4°C FACS buffer (3% FBS in PBS) and smashed in a cell strainer (100 mm Nylon, BD Falcon). Cell suspensions were treated with lysis buffer (0.15M NH_4Cl, 1 mM $NaHCO_3$, 0.1 mM EDTA) for 6 minutes on ice and washed 3 times with cold FACS buffer. Cells were finally suspended in FACS buffer and used for ELISpot or flow cytometry. Immune cell populations were detected with fluorescently labeled antibodies as follows. Plasma cells (CD138+k-light chain+): FITC-rat, anti mouse k-light chain (BD pharmigen) and PE-rat, anti-mouse CD138 (BD pharmigen). Germinal center B cells (B220+GL7+): APC-rat, anti-mouse B220 (eBioscience) and biotin-rat, anti- mouse GL-7 (BD pharmigen) followed by incubation with pacific blue conjugated Streptavidin-peridinin chlorophyII A (SA-PB, Invitrogen). Memory B cells (CD4/CD8/F4/80-IgD-CD19+IgG+CD38+): PE-rat, anti-mouse IgD, biotin-rat, anti-mouse CD19, FITC-rat, anti-mouse IgG1/IgG2a2b and PeCy5-rat, anti-mouse CD38. A combination of PeCy7-rat, anti-mouse CD4- CD8- and F4/80 were used to exclude non-B cells. Biotin-labeled antibodies were detected with SA-PB (Invitrogen).

Enzyme-linked immunospot (ELISpot) assay for antibody-secreting cells

ELISpot was performed as described previously (29, 30). Briefly, in order to detect anti-dsDNA-secreting cells, 96-well MultiScreen plates (Millipore) were coated with poly-L-lysine and incubated with calf thymus DNA. Plates were coated with goat anti-mouse IgG (Fc fragment specific, Jackson ImmunoResearch Laboratories) to detect total IgG-secreting cells. Cell suspensions from spleen, bone marrow and kidney were added to individual wells, starting with $5X10^5$ cells in the top row. Cells were incubated overnight at 37°C, in a 5% CO_2 atmosphere. After incubation, plates were washed several times with 0.1% Tween 20 in PBS, incubated with alkaline phosphatase-goat, anti-mouse IgG antibody (Southern Biotech) and finally developed with vector blue alkaline phosphatase substrate III kit (Vector Laboratories). Antibody-secreting cells were enumerated with an ELISpot Scanner (Cellar Technology Ltd.).

Enzyme-linked immunosorbent assay

Blood from experimental mice (control and treated groups) was collected, centrifuged and serum was stored at −80°C until quantification of antibody levels. Anti-dsDNA, IgG concentration was determined with a commercial, mouse anti-dsDNA kit from Alpha Diagnostic International according to manufacturer's recommendations. Total IgG and IgM levels were quantified according to a previously described standard ELISA protocol (Frederick Ausubel, Current Protocol in Molecular Biology, 11.2.1).

Immunofluorescent analysis

4 μm frozen sections were blocked for 30 minutes with 5% donkey serum (Jackson Immunoresearch Laboratories, 017-000-121) and Fc block (BioXcell, 10 μg/ml, 2.4G2) to prevent non-specific binding. Without washing, primary antibodies, dissolved in PBS, were added to the tissue section and incubated in a humid chamber for 30 minutes at room temperature. Slides were briefly washed in PBS and fluorochrome-conjugated, secondary antibodies or fluorescently labeled streptavidin (SA) were added to the tissues to visualize primary antibodies. Briefly, to detect germinal centers and isotype-switched ASC, frozen spleen sections were incubated with PE-rat, anti-mouse IgD (eBioscience, clone 11-26), biotin-donkey, anti-mouse IgG (Jackson Immunoresearch Laboratories, 715-066-150) and FITC-peanut agluttinin (SIGMA, L7381). Rabbit anti-PE (Rockland Immunochemicals, 200-4199) and Cy-3-donkey, anti-rabbit (Jackson Immunoresearch Laboratories, 711-165-152) were used to detect IgD+ cells and Streptavidin-Cy5 (eBioscience, 19-4317-82) to visualize IgG+ cells, respectively. To detect FDC networks, T cells and B cell follicles, spleen sections were first incubated with biotin-rat, anti-mouse CD21-CD35 (Biolegend, clone 7E9), purified anti mouse CD3 (Santa Cruz Biotechnology, clone M-20) and APC-CD45R (B220, BD Pharmingen, clone RA3-6B2). After incubation with primary antibodies, FDC were detected with SA-Alexa fluor 488 (Invitrogen, S-32354) and T cells were detected with Alexa fluor 568, donkey anti-goat (Invitrogen, A11057). Frozen kidney sections were incubated with BR3-Fc human fusion protein, biotinylated anti-alpha, smooth muscle actin (Neomarkers, clone 1A4) and FITC-rat anti-mouse IgG (BD Pharmingen). Incubation with primary antibodies was followed by incubation with Cy-3 donkey anti human IgG (Jackson Immunoresearch Laboratories, 709-166-149) to detect BAFF and SA-Cy5 (eBioscience, 19-4317-82) to visualize IgG deposition. PE-rat anti-mouse CD256/APRIL (Biolegend, clone A3D8), FITC-anti mouse/human CXCL12 (R&D systems, IC350F) and purified rat, anti-mouse F4/80 (AbD Serotec, MCA497GA), in combination with rabbit anti-PE (Rockland Immunochemicals, 200-4199), Cy-3 donkey anti-rabbit (Jackson Immunoresearch Laboratories, 711-165-152), biotin-donkey anti rat (Jackson Immunoresearch Laboratories, 712-066-150) and Streptavidin-Cy5 (eBioscience, 19-4317-82) were used to detect April, CXCL12 and F4/80+ macrophages. Slides were washed in PBS for 3 hours and mounted with Slow Fade Gold Antifade with DAPI (Invitrogen, S36938). T cells were pseudocolored white. Representative pictures were taken with a Zeiss Axioplan Microscope and recorded with a Zeiss Axiocam digital camera. For morphometric analysis, all the PNA^+ germinal centers in spleens and IgG^+ deposition areas in the kidneys were outlined with the automated tool of the Carl Zeiss Microscope. Due to the different size of frozen tissue sections, we calculated the percentages of area occupied by GC and IgG deposition by dividing the total area occupied by GC or IgG+ signal by the total area of the tissue section.

Quantitative PCR

Ten, 30 μm thick, frozen tissue slices were collected in TRIzol (Invitrogen) and homogenized with a DNAse and RNAse free pipette tip. 5 μg of Glycogen (Ambion, AM9510) was added to the sample in TRIzol to increase RNA yield. RNA isolation was performed according to the TRIzol protocol, and total RNA was quantified in the Nanodrop. 3 μg of total RNA were reverse transcribed using random primers and superscript II. cDNA concentration was adjusted to 10 ng/μl and 50 ng of cDNA were used per PCR reaction. PCR reaction was performed in a Step One plus ABI machine, using Applied biosystems commercial probes for Gapdh (Mm9999915_g1), Bcl6 (Mm00477633_m1), Cxcl12 (Mm00445553_m1), April (Mm03809849_s1), Baff Mm00446347_m1) and Il6 (Mm00446190_m1) and according to the ABI protocol. To calculate changes in mRNA expression, mRNA expression was first normalized to Gapdh mRNA expression and mRNA expression for each gene in the experimental groups was compared to the level of mRNA

expression in Balb/c mice or younger NZB/NZW F1 mice. Fold changes in mRNA expression were calculated according to the 'ΔΔCT' calculation (change in cycling threshold) recommended by Applied Biosystems.

Statistical analysis

All data were analyzed under GraphPad Prism5 software. Mann-Whitney *test* and student *t-test* were applied for comparing differences among experimental groups. A value of $p \leq 0.05$ was considered statistically significant.

RESULTS

Progressive increase in ASCs correlates with systemic levels of circulating auto-antibodies and accumulation of dsDNA-specific, PC in the inflamed kidney of SLE prone mice

We previously demonstrated that antibody-secreting cells (ASC) specific for IgG or dsDNA were dramatically increased in spleen and moderately increased in BM from NZB/W mice with lupus nephritis (29). To better define the correlation between systemic levels of autoantibodies and progressive generation of ASCs in different anatomical compartments, we enumerated ASCs in spleen, BM and kidney from NZB/W mice, collected at different ages. In 8 week old pre-disease NZB/W mice, total IgG ASCs were detected in the spleen and BM, but they were undetectable in the kidney (Figure 1A), consistent with the findings reported in previous studies (25). In the spleen and kidney, there was a clear correlation among the increase in the number of isotype-switched PCs, the age-associated disease progression, and the levels of circulating IgG autoantibodies. In the BM, similar numbers of total IgG ASCs were detected in all groups, except in NZB/W mice with high autoantibody titers.

In contrast, dsDNA-specific ASCs were absent in the spleen, BM and kidney at 8 week of age (Figure 1B). Considerable numbers of dsDNA+ ASCs were first detected in the spleen (19 wk) and progressively increased in all three organs peaking at 39 wk. Confirming previous reports (26, 31), numbers of renal IgG- and dsDNA-specific ASCs increased significantly in 39 week NZB/W F1 mice, especially those with high titers of anti-dsDNA antibodies (Figure 1A and 1B). This supports the idea that the inflamed kidney offers a unique survival niche for plasma cells (31). The ratio of anti-dsDNA/anti-IgG ASCs in the inflamed kidney (31.4%±3.7%) was 10-fold higher than in spleen (3.17%±0.25%) and BM (2.43%±0.26%) in high-dsDNA antibody mice (Figure 1C).

Spontaneous formation of splenic GCs contributes to isotype-switched PC generation in SLE

A hallmark of SLE is the spontaneous formation of germinal centers, which are an important source of auto-reactive plasma cells. Based on the early detection of considerable numbers of auto-reactive ASCs in spleen, followed by the progressive accumulation of ASCs in the BM and kidney, we hypothesized that a large proportion of auto-reactive PCs were generated in the spleen and preferentially migrate to the inflamed kidneys. In order to visualize the kinetics of GC formation in NZB/W mice, we stained spleen frozen sections, collected at different ages, with antibodies against follicular dendritic cells (FDC), T cells, and GC B cells. We observed a progressive increase in the organizational complexity of FDC networks together with accumulation of T cells inside the GC (Figure 2A). To definitively analyze the temporal formation of GC and the generation of GC-derived PCs, we stained with antibodies against IgD (to identify naïve B cells and delineate the follicular B cell zone) and IgG (to detect isotype-switched plasma cells), in combination with fluorescently labeled peanut agglutinin (to visualize GC B cells) (Figure 2B). There was an

increase in the size and number of GCs as NZB/W mice aged, with a 3-fold increase in GC area at 19 week and a 7–8-fold increase at 39 week (Figure 2C).

At an early age (8 week), IgG^+ PCs were very rare with the majority located inside the GC. By 19 week, there was a modest increase in the number of IgG^+ PCs located either in the GC or in the extra-follicular zone. The location of IgG^+ PCs in close association with large $IgD^-B220^+PNA^+$ GC B cells suggests that they were mainly derived from the GC. Finally at 39 week, numerous IgG^+ PCs were found in both the GC and the extra-follicular regions of the spleen (Figure 2D). These results suggest that in experimental SLE, disease progression is associated with an increase in the number and size of GCs, which are likely the main source of isotype-switched PCs.

Increase in PC survival factors in lupus prone mice

Next we assessed the kinetics of mRNA expression for survival factors (BAFF, APRIL, IL6) and chemokines (CXCL12) that participate in the survival and recruitment of PCs to specialized niches in secondary lymphoid organs and inflamed tissues. Although IL6 induces the terminal differentiation of B cells into PC and it is important for PC survival (32), IL6 mRNA expression was stable until 39 weeks, at which time a 4-fold increase was observed. APRIL mRNA expression showed a modest increase, and interestingly CXCL12 mRNA expression progressively declined in the spleen tissue (Figure 3A). In addition, we measured mRNA expression for Bcl-6, the master transcription factor for GC B cells and TFH cells, which are both critical players in PC production. Bcl-6 also participates in B cell proliferation, antibody class switching, affinity maturation and is critical for differentiation of naïve B cells into plasma cells (33). In the spleen, we observed a modest but progressive increase in mRNA expression for Bcl-6 (data not shown).

In the inflamed kidney, IL6 mRNA expression mirrored its expression in the spleen, dramatically increasing at 39 weeks. BAFF and APRIL increased modestly in the kidney (Figure 3B). Notably, the protein expression of IL6, BAFF, and APRIL in the kidney was also increased in lupus compared to control mice (Figure 3C). Although mRNA expression of CXCL12 remained constant, CXCL12 protein expression increased significantly in the kidney (Figure 3C), following an opposite trend compared to the spleen. Overall, increased production of survival factors for PCs in both the spleen and inflamed kidneys suggests that auto-reactive PCs successfully find survival niches in both anatomical locations. A reduction in CXCL12 mRNA expression in the spleen, coupled with its increased expression in the kidney implicates a chemokine gradient in promoting the selective movement of auto-reactive plasma cells from the spleen to the inflamed kidney.

Short-term BCD with anti-mCD20 antibody does not impact ASCs

In order to better understand the impact of B cell depletion therapy on PC kinetics and longevity, we decided to model the effects of short-term anti-CD20 treatment on PC accumulation in different anatomical compartments. Short-term therapy with anti-CD20 neither reduced the numbers of IgG- or dsDNA specific ASCs (spleen, BM and inflamed kidney) (Figure 4A and 4B) (29) nor the ratio of anti-dsDNA ASCs/anti-IgG ASC (Figure 4C). One potential explanation for the failure of short-term, anti-CD20 treatment to deplete auto-reactive PCs is the lack of expression of CD20 on PCs. However, if PCs are short-lived one would expect them to subsequently decline over time if B cell depletion is effective. To test this possibility, we enumerated auto-reactive PC in a group of mice that received BCD therapy for 4 consecutive weeks, followed for an 8 weeks resting period. Similar to short-term depletion, we did not observe any differences in the numbers of auto-reactive PCs in spleen, BM, and kidney (Figure 4; see 4wks/8wks point).

Long-term BCD significantly reduces ASCs with dramatic effects on auto-reactive cells in kidney

In contrast to short-term BCD therapy, prolonged treatment with anti-CD20 caused a significant reduction in the number of IgG- and dsDNA specific ASC in the spleen (>100-fold reduction: anti-IgG ASCs, >60 fold reduction: anti-dsDNA IgG ASCs) (Figure 4A and 4B). Although IgG- and dsDNA specific ASCs were only modestly decreased in the BM (2.7-fold and 5.5-fold), the reduction in auto-reactive PCs was still statistically significant. However, the ratio of dsDNA specific ASC/IgG specific ASC in the spleen and BM did not significantly change (Figure 4C). Given the enrichment of auto-reactive PCs in the inflamed kidney, we also analyzed the impact of long-term BCD therapy on the numbers of auto-reactive PCs in this location. Total IgG ASCs in kidney from treated mice were modestly reduced (control: $5.94\pm0.53\times10^4$/kidney, 12 week treatment: $1.72\pm0.08\times10^4$/kidney) (Figure 4A and 4B). However, a more pronounced impact was noted on renal anti-dsDNA ASCs (15 fold reduction; control: $1.16\pm0.06\times10^3$/kidney vs 12 week treatment: $0.074\pm0.013\times10^3$/kidney). Finally, the ratio of dsDNA specific ASC/IgG specific ASC in treated mice declined 6.8-fold compared to control group (control: 27.3±3.7%, treated mice: 3.98±0.73%, p=0.022). Correspondingly, serum anti-dsDNA antibody levels also declined with prolonged treatment (Figure 4D) (p=0.0095 control vs 12 wk treatment). Overall these results suggest that splenic- and renal ASCs can be effectively targeted by long-term BCD therapy, but this is unlikely to be mediated by CD20 expression on their surface or the gradual disappearance of short-lived PCs. In addition, prolonged BCD suppressed the progression of nephritis [Mean±SEM of proteinuria (0–4+) 3.17±0.19 in control (n=6) vs 1.17±0.17 in 12 wks treatment (n=6) (p=0.012)].

Long-term BCD therapy efficiently reduces B cells and GCs in the spleen

One mechanistic explanation for the reduction of auto-reactive PC after long-term BCD therapy is the more efficient elimination of B cells before or during differentiation in the GC. To explore this hypothesis, we analyzed the impact of long-term BCD on B cell numbers, GC differentiation, and spatial distribution by flow cytometry and immunofluorescence. In agreement with previous reports (34, 35), short-term treatment was effective in depleting $B220^+$ B cells but had less impact on GL-7^+B220^+ GC B cells. The duration of B cell depletion after short-treatment was temporary because numbers of B cells returned to control levels in the group treated for 4 weeks and allowed to reconstitute for 8 weeks. In sharp contrast, long-term BCD therapy had a profound effect on both $B220^+$ B cells and $B220^+GL\text{-}7^+$ GC B cells (Figure 5A). Detection of clusters of large $IgD^-B220^+PNA^+$ cells by immunofluorescence showed that GCs disappeared or shrank substantially 12 weeks after anti-CD20 treatment. Conversely, GCs were still intact in mice receiving BCD therapy for only 4 weeks (Figure 5C). Overall, these results suggest that long-term BCD therapy is required to efficiently eliminate GC B cells and interfere with the generation of GC-derived auto-reactive PCs in the spleen of lupus prone mice.

Plasma cells decrease after long-term BCD treatment

To investigate the impact of prolonged anti-mCD20 antibody therapy on the PC population, we enumerated $CD138^+\kappa$ light $chain^+$ cells by flow cytometry. Only long-term BCD therapy induced a statistically significant 10-fold reduction in the number of splenic PCs. Neither short-term nor long-term BCD had a significant impact on the population of quiescent long-lived, PCs in the BM (Figure 5B). Interactions of B cells with stromal cell populations are critical for maintaining the architecture of secondary lymphoid organs. Visual examination of spleen sections stained with antibodies against FDC (CD21-CD35), T cells (CD3) and B cells (B220), revealed the control group contained numerous and well-organized GCs with dense $CD21\text{-}CD35^+$ FDC networks, $CD3^+$ T cell infiltrates, large clusters of

$IgD^{-}B220^{+}PNA^{+}$ GC B cells and follicular and extra-follicular IgG^{+} PC. Short-term treatment with anti-CD20 depletion resulted in a reduction in the size of GCs, impaired T cell infiltration inside GC, and promoted enlargement of the T cell zone. However, GC organization and the presence of PCs were still evident after short-term BCD for 4 weeks. In the group that experience reconstitution after treatment for 4 weeks with anti-CD20 and 8 week rest, there was recovery in the size and organization of B cell follicles and GC, more T cells were detected inside the GC, and the FDC networks began to acquire their classic concentric and dense distribution. Long-term treatment with anti-CD20 resulted in a remarkable shrinkage of the B cell follicles and FDC networks (Figure 5C). Additionally, there was a significant decrease in isotype-switched, IgG^{+} plasma cells on morphometric analysis (IgG+ PC#/200x HPF mean±SEM: Ctr 65.3±4.8, 4 week 58.5±2.5, 4/8 week 52.9±4.9, 12 week 26.8±1.5, p=0.0001 for unpaired t-test comparison between 12 week and other groups).

BCD increases the expression of PC survival factors in spleen but decreases expression in the inflamed kidney

To determine whether long-term BCD therapy modulated the expression of survival factors for PCs (32, 36), we examined mRNA expression for CXCL12, IL6, BAFF, and APRIL by quantitative PCR. Interestingly, both long-term- and short-term BCD therapy increased the expression of BAFF and APRIL in the spleen (Figure 6A). Although we were predicting that B cell depletion would lead to an increase in available BAFF protein, an increase in BAFF and APRIL mRNA expression was unexpected. This suggests that B cells are required to modulate the production of BAFF and APRIL in the spleen and/or that increased expression of both survival factors is a compensatory mechanism to induce the rapid recovery of B cells. BCD also induced an increase in mRNA expression for CXCL12 and IL6 in the spleen (Figure 5A). Given that CXCL12 and IL6 are required for PC survival (32), an increase in expression in the spleen after BCD may contribute to the maintenance of PCs in this location. In contrast to results in the spleen, we found that mRNA levels for BAFF, APRIL and IL6 were significantly reduced in the kidney after both short-term and long-term BCD therapy (Figure 6B). CXCL12 mRNA expression was unchanged although notably not increased (Figure 6B).

To more directly characterize the PC niche in the kidney and the impact of BCD, we next examined the protein expression and cellular localization of survival factors implicated in PC survival. In control mice, BAFF was expressed predominantly in glomeruli (Figure 6C Ctrl panel on left and magnified image) and was dramatically reduced to undetectable levels after BCD (see quantitation in Figure 6D), correlating with the PCR data. In marked contrast, BAFF expression was unchanged in mice treated with short-term BCD therapy (Figure 6D). APRIL was preferentially produced by stromal cells in and around inflamed glomeruli (Figure 6C Ctrl panel on right) and was significantly decreased with long-term BCD but only modestly changed with short-term treatment. Both treatment groups displayed a reduction in IL6 and CXCL12 expression (Figure 6D). Both stromal cells and F4/80+ macrophages (37) in the inflamed kidney were prime producers of CXCL12 (Figure 6C). Notably, F4/80+ macrophages were significantly decreased but after only after long-term BCD (see quantitation in Figure 6D). These findings suggest that macrophages and stromal cells contribute to homing and survival of plasma cells in the inflamed kidney, and BCD alters this niche, by decreasing the numbers of macrophages and the expression of key cytokines and chemokines.

DISCUSSION

This study explored the generation and maintenance of auto-reactive plasma cells in murine lupus and the impact of B cell depletion therapy. Anti-dsDNA PCs were rapidly enriched in

the kidney after generation in GC reactions in the spleen, concurrent with the development of serum autoantibodies and preceding the onset of frank nephritis. Auto-reactive PCs further accumulated in the kidney with disease progression coincident with an increase in renal expression of key PC survival factors (BAFF, APRIL and IL6) and PC attracting chemokines (CXCL12). Although short-term anti-CD20 treatment suppressed the progression of nephritis, ASCs in multiple organs were not significantly impacted even after a prolonged period of time elapsed between treatment and follow-up (8 weeks). In marked contrast, long-term BCD with anti-CD20 (12 weeks) dramatically reduced ASCs in the spleen and kidney, with particularly notable effects on auto-reactive PCs in the kidney. The reduction in PCs in the kidney was accompanied by decreases in PC survival factors and PC attracting chemokines, suggesting that B cell depletion can alter the PC survival niche.

The accumulation of auto-antibody secreting cells and long-lived plasma cells in the kidneys of lupus-prone mice has been recently described (25, 26). However, our results detail for the first time the kinetics of this process and suggest a role for specific soluble factors (BAFF, APRIL, CXCL12, IL6) in establishing a PC survival niche. Since GC B cells have not been readily detected in the kidney, it was proposed that auto-reactive PCs are generated in secondary lymphoid organs such as spleen and migrate into kidney, finding survival niches (26, 31). Indeed, in our experiments spontaneous GCs were first noted at 8 weeks in the spleen of lupus-prone mice and increased further at the onset of serum auto-antibody production (19 weeks) and nephritis progression (39 weeks). This correlated with an increase in Bcl-6 first noted at 8 weeks, notable given that it is a key transcription factor for GC B cells and TFH cells, both critical players in GC reactions and PC production (33). Another factor that enhances B cell differentiation to PC is IL6 (38), but this was significantly enriched in the splenic microenvironment only in older diseased mice (39 week old). In contrast, the PC survival factor APRIL was increased even pre-disease onset similar to Bcl-6. Notably, in the kidney of older lupus prone mice the protein expression of multiple PC survival factors including BAFF, APRIL, IL6, and CXCL12 was increased. Although we find active immune responses in the spleen of lupus-prone mice with numerous active GC reactions and ongoing PC generation, it remains possible that PCs also arise within the kidney. Indeed, a recent study in human lupus nephritis described GC and T:B aggregate in the renal tubulo-interstitium. Moreover, B cell proliferation and somatic hypermutation were ongoing, implicating the kidney as a site of active immune responses and source of PCs (39).

The other notable finding in our study is the impact of long-term BCD on ASCs in the kidney, spleen, and BM. We propose two mechanisms for this effect: 1) decreased generation of new PCs via interruption of GC reactions in the spleen and 2) disruption of the PC survival niche that contributes to the maintenance of long-lived PCs. It has been previously shown that anti-CD20 effectively depletes marginal zone, GC, and memory B cells but does not decrease long-lived antibody levels, suggesting that memory B cell subsets are not necessary for maintaining antibody levels (27, 28). However, in autoimmunity there may be some resistance of B cell subsets to depletion in both mice (29, 34) and humans (15, 40). Our data suggests that prolonged treatment with anti-CD20 may overcome this effect. Although auto-reactive ASCs decreased in all tissues with prolonged BCD, there was differential sensitivity with effects in the kidney more pronounced than spleen and BM. Only in the kidney was the high ratio of anti-dsDNA IgG ASC to total IgG ASCs decreased. This could be because the frequency of long-lived vs. short-lived PCs varies in the different tissues. For example, in NZB/W mice up to 40% of splenic PCs are long-lived (21), whereas this frequency is even higher in the BM (41). Short-lived plasma cells (plasmablasts) can still express low levels of CD20 (42) and thus may be directly targeted by anti-CD20. Alternatively, thorough depletion of precursor B cells and interruption of ongoing PC generation should ultimately decrease short-lived PCs.

An additional explanation for the impact of prolonged BCD on auto-reactive ASCs is an alteration in the niche affecting the survival of long-lived PCs. Many factors are required for B cell differentiation to PC (IL6), homing to the PC niche (CXCL12), and PC survival (BAFF, APRIL) (43, 44). In BAFF KO and APRIL KO mice, PCs in BM are profoundly decreased (45). On the other hand, once a long-lived PC pool is established in the BM blockade of both BAFF and APRIL and other factors may be necessary to deplete long-lived PCs (22). Thus, blockade of BAFF or APRIL decreased auto-reactive PCs in the spleen and BM of lupus-prone mice (46), but combined BAFF/APRIL blockade had a greater impact on total IgG ASC in the BM (46) and the frequency of PCs in the spleen (47). The impact of such therapy on renal PCs has not been studied although activated renal macrophages did decrease (46). Here we find that BM total IgG ASCs and anti-dsDNA ASCs were slightly although significantly reduced with prolonged BCD, with more pronounced effects in the spleen and even more significant effects in the kidney. Interestingly, PC survival factors including BAFF and APRIL were dramatically decreased by long-term but not short-term BCD.

A major question is how B cell depletion alters PC survival and migration factors in the kidney. We found that macrophages producing APRIL and CXCL12 in the kidney were significantly decreased and BAFF production was abrogated with prolonged BCD, suggesting for the first time that BCD may alter the PC survival niche by impacting infiltrating and resident cells in the kidney that produce key PC survival factors and chemo-attractants. This is in accord with published data demonstrating an accumulation of activated renal macrophages in the kidney in murine lupus nephritis (48), but therapeutic targeting of these pathways has not been previously demonstrated. These effects are likely critical to the beneficial impact of prolonged BCD given that PCs in the inflamed kidney in murine lupus nephritis appear to be long-lived based on phenotype and BrdU labeling (25, 26). We speculate that splenic and BM PC niches are not impacted by BCD in the same way as the kidney given that decreases in ASCs in these locations were more modest. A recent study in human immune thrombocytopenia (ITP) found that splenic PCs after BCD acquired a long-lived gene expression signature similar to BM PCs and were resistant to rituximab (49). This may be mediated by increases in BAFF and APRIL in the setting of BCD as we have demonstrated here.

In summary, our experiments show that the inflamed kidney is a site for enrichment of long-lived plasma cells, a compartment notoriously difficult to target. Although short-term BCD with anti-CD20 had no significant effect on ASCs, long-term BCD significantly reduced ASCs in the spleen, BM, and kidney by both interrupting the ongoing generation of short-lived PCs in the spleen and altering the long-lived PC niche in the kidney. The results provide important information about BCD and the factors regulating the survival of PCs, with critical implications for the treatment of autoimmune disease.

Acknowledgments

We acknowledge Biogen Idec for provision of the murine anti-CD20 antibody.

Abbreviations

dsDNA	double-stranded DNA
PC	plasma cell
SLE	systemic lupus erythematosus
BCD	B cell depletion

GC	germinal center
ASC	antibody-secreting cell
BM	bone marrow
APRIL	a proliferation-inducing ligand
BAFF	B cell activator of the TNF family

References

1. Anolik JH. B cell biology and dysfunction in SLE. Bulletin of the NYU hospital for joint diseases. 2007; 65:182–186. [PubMed: 17922667]
2. Chan O, Shlomchik MJ. A new role for B cells in systemic autoimmunity: B cells promote spontaneous T cell activation in MRL-lpr/lpr mice. J Immunol. 1998; 160:51–59. [PubMed: 9551955]
3. Shlomchik MJ, Madaio MP, Ni D, Trounstein M, Huszar D. The role of B cells in lpr/lpr-induced autoimmunity. The Journal of experimental medicine. 1994; 180:1295–1306. [PubMed: 7931063]
4. Martin F, Chan AC. Pathogenic roles of B cells in human autoimmunity; insights from the clinic. Immunity. 2004; 20:517–527. [PubMed: 15142521]
5. Chan OT, Hannum LG, Haberman AM, Madaio MP, Shlomchik MJ. A novel mouse with B cells but lacking serum antibody reveals an antibody-independent role for B cells in murine lupus. The Journal of experimental medicine. 1999; 189:1639–1648. [PubMed: 10330443]
6. Harris DP, Haynes L, Sayles PC, Duso DK, Eaton SM, Lepak NM, Johnson LL, Swain SL, Lund FE. Reciprocal regulation of polarized cytokine production by effector B and T cells. Nature Immunology. 2000; 1:475–482. [PubMed: 11101868]
7. Anolik JH, Looney RJ, Lund FE, Randall TD, Sanz I. Insights into the heterogeneity of human B cells: diverse functions, roles in autoimmunity, and use as therapeutic targets. Immunol Res. 2009
8. Bave U, Alm GV, Ronnblom L. The combination of apoptotic U937 cells and lupus IgG is a potent IFN-alpha inducer. Journal of Immunology. 2000; 165:3519–3526.
9. Leadbetter EA, Rifkin IR, Hohlbaum AM, Beaudette BC, Shlomchik MJ, Marshak-Rothstein A. Chromatin-IgG complexes activate B cells by dual engagement of IgM and Toll-like receptors.[see comment]. Nature. 2002; 416:603–607. [PubMed: 11948342]
10. Means TK, Latz E, Hayashi F, Murali MR, Golenbock DT, Luster AD. Human lupus autoantibody-DNA complexes activate DCs through cooperation of CD32 and TLR9. J Clin Invest. 2005; 115:407–417. [PubMed: 15668740]
11. Viglianti GA, Lau CM, Hanley TM, Miko BA, Shlomchik MJ, Marshak-Rothstein A. Activation of autoreactive B cells by CpG dsDNA. Immunity. 2003; 19:837–847. [PubMed: 14670301]
12. Lambert PH, Dixon FJ. Pathogenesis of the glomerulonephritis of NZB/W mice. The Journal of experimental medicine. 1968; 127:507–522. [PubMed: 4169964]
13. Winfield JB, Faiferman I, Koffler D. Avidity of anti-DNA antibodies in serum and IgG glomerular eluates from patients with systemic lupus erythematosus. Association of high avidity antinative DNA antibody with glomerulonephritis. J Clin Invest. 1977; 59:90–96. [PubMed: 299748]
14. Waldman M, Madaio MP. Pathogenic autoantibodies in lupus nephritis. Lupus. 2005; 14:19–24. [PubMed: 15732283]
15. Looney RJ, Anolik JH, Campbell D, Felgar RE, Young F, Arend LJ, Sloand JA, Rosenblatt J, Sanz I. B cell depletion as a novel treatment for systemic lupus erythematosus: a phase I/II dose-escalation trial of rituximab. Arthritis and rheumatism. 2004; 50:2580–2589. [PubMed: 15334472]
16. Smith KG, Jones RB, Burns SM, Jayne DR. Long-term comparison of rituximab treatment for refractory systemic lupus erythematosus and vasculitis: Remission, relapse, and re-treatment. Arthritis and rheumatism. 2006; 54:2970–2982. [PubMed: 16947528]
17. Edwards JC, Leandro MJ, Cambridge G. B-lymphocyte depletion therapy in rheumatoid arthritis and other autoimmune disorders. Biochem Soc Trans. 2002; 30:824–828. [PubMed: 12196207]

18. Anolik JH, Barnard J, Owen T, Zheng B, Kemshetti S, Looney RJ, Sanz I. Delayed memory B cell recovery in peripheral blood and lymphoid tissue in systemic lupus erythematosus after B cell depletion therapy. Arthritis and rheumatism. 2007; 56:3044–3056. [PubMed: 17763423]
19. Sabahi R, Anolik JH. B-cell-targeted therapy for systemic lupus erythematosus. Drugs. 2006; 66:1933–1948. [PubMed: 17100405]
20. Merrill JT, Neuwelt CM, Wallace DJ, Shanahan JC, Latinis KM, Oates JC, Utset TO, Gordon C, Isenberg DA, Hsieh HJ, Zhang D, Brunetta PG. Efficacy and safety of rituximab in moderately-to-severely active systemic lupus erythematosus: the randomized, double-blind, phase II/III systemic lupus erythematosus evaluation of rituximab trial. Arthritis and rheumatism. 62:222–233. [PubMed: 20039413]
21. Hoyer BF, Moser K, Hauser AE, Peddinghaus A, Voigt C, Eilat D, Radbruch A, Hiepe F, Manz RA. Short-lived plasmablasts and long-lived plasma cells contribute to chronic humoral autoimmunity in NZB/W mice. The Journal of experimental medicine. 2004; 199:1577–1584. [PubMed: 15173206]
22. Winter O, Dame C, Jundt F, Hiepe F. Pathogenic long-lived plasma cells and their survival niches in autoimmunity, malignancy, and allergy. J Immunol. 2012; 189:5105–5111. [PubMed: 23169863]
23. Sekine H, Watanabe H, Gilkeson GS. Enrichment of anti-glomerular antigen antibody-producing cells in the kidneys of MRL/MpJ-Fas(lpr) mice. J Immunol. 2004; 172:3913–3921. [PubMed: 15004199]
24. Lacotte SH, Dumortier H, Decossas M, Briand JP, Muller S. Identification of new pathogenic players in lupus: autoantibody-secreting cells are present in nephritic kidneys of (NZBxNZW)F1 mice. J Immunol. 184:3937–3945. [PubMed: 20181885]
25. Starke C, Frey S, Wellmann U, Urbonaviciute V, Herrmann M, Amann K, Schett G, Winkler T, Voll RE. High frequency of autoantibody-secreting cells and long-lived plasma cells within inflamed kidneys of NZB/W F1 lupus mice. Eur J Immunol. 41:2107–2112. [PubMed: 21484784]
26. Espeli M, Bokers S, Giannico G, Dickinson HA, Bardsley V, Fogo AB, Smith KG. Local renal autoantibody production in lupus nephritis. J Am Soc Nephrol. 22:296–305. [PubMed: 21088295]
27. DiLillo DJ, Hamaguchi Y, Ueda Y, Yang K, Uchida J, Haas KM, Kelsoe G, Tedder TF. Maintenance of long-lived plasma cells and serological memory despite mature and memory B cell depletion during CD20 immunotherapy in mice. J Immunol. 2008; 180:361–371. [PubMed: 18097037]
28. Ahuja A, Anderson SM, Khalil A, Shlomchik MJ. Maintenance of the plasma cell pool is independent of memory B cells. Proceedings of the National Academy of Sciences of the United States of America. 2008; 105:4802–4807. [PubMed: 18339801]
29. Bekar KW, Owen T, Dunn R, Ichikawa T, Wang W, Wang R, Barnard J, Brady S, Nevarez S, Goldman BI, Kehry M, Anolik JH. Prolonged effects of short-term anti-CD20 B cell depletion therapy in murine systemic lupus erythematosus. Arthritis and rheumatism. 2010; 62:2443–2457. [PubMed: 20506300]
30. Ichikawa HT, Conley T, Muchamuel T, Jiang J, Lee S, Owen T, Barnard J, Nevarez S, Goldman BI, Kirk CJ, Looney RJ, Anolik JH. Beneficial effect of novel proteasome inhibitors in murine lupus via dual inhibition of type I interferon and autoantibody-secreting cells. Arthritis and rheumatism. 2012; 64:493–503. [PubMed: 21905015]
31. Cassese G, Lindenau S, de Boer B, Arce S, Hauser A, Riemekasten G, Berek C, Hiepe F, Krenn V, Radbruch A, Manz RA. Inflamed kidneys of NZB / W mice are a major site for the homeostasis of plasma cells. Eur J Immunol. 2001; 31:2726–2732. [PubMed: 11536171]
32. Cassese G, Arce S, Hauser AE, Lehnert K, Moewes B, Mostarac M, Muehlinghaus G, Szyska M, Radbruch A, Manz RA. Plasma cell survival is mediated by synergistic effects of cytokines and adhesion-dependent signals. J Immunol. 2003; 171:1684–1690. [PubMed: 12902466]
33. Basso K, Dalla-Favera R. BCL6: master regulator of the germinal center reaction and key oncogene in B cell lymphomagenesis. Advances in immunology. 2010; 105:193–210. [PubMed: 20510734]
34. Ahuja A, Shupe J, Dunn R, Kashgarian M, Kehry MR, Shlomchik MJ. Depletion of B cells in murine lupus: efficacy and resistance. J Immunol. 2007; 179:3351–3361. [PubMed: 17709552]

35. Gong Q, Ou Q, Ye S, Lee WP, Cornelius J, Diehl L, Lin WY, Hu Z, Lu Y, Chen Y, Wu Y, Meng YG, Gribling P, Lin Z, Nguyen K, Tran T, Zhang Y, Rosen H, Martin F, Chan AC. Importance of cellular microenvironment and circulatory dynamics in B cell immunotherapy. J Immunol. 2005; 174:817–826. [PubMed: 15634903]
36. Fairfax KA, Kallies A, Nutt SL, Tarlinton DM. Plasma cell development: from B-cell subsets to long-term survival niches. Seminars in immunology. 2008; 20:49–58. [PubMed: 18222702]
37. Schiffer L, Bethunaickan R, Ramanujam M, Huang W, Schiffer M, Tao H, Madaio MP, Bottinger EP, Davidson A. Activated renal macrophages are markers of disease onset and disease remission in lupus nephritis. J Immunol. 2008; 180:1938–1947. [PubMed: 18209092]
38. Hirano T, Taga T, Nakano N, Yasukawa K, Kashiwamura S, Shimizu K, Nakajima K, Pyun KH, Kishimoto T. Purification to homogeneity and characterization of human B-cell differentiation factor (BCDF or BSFp-2). Proceedings of the National Academy of Sciences of the United States of America. 1985; 82:5490–5494. [PubMed: 2410927]
39. Chang A, Henderson SG, Brandt D, Liu N, Guttikonda R, Hsieh C, Kaverina N, Utset TO, Meehan SM, Quigg RJ, Meffre E, Clark MR. In situ B cell-mediated immune responses and tubulointerstitial inflammation in human lupus nephritis. J Immunol. 2011; 186:1849–1860. [PubMed: 21187439]
40. Anolik JH, Barnard J, Cappione A, Pugh-Bernard AE, Felgar RE, Looney RJ, Sanz I. Rituximab improves peripheral B cell abnormalities in human systemic lupus erythematosus. Arthritis Rheum. 2004; 50:3580–3590. [PubMed: 15529346]
41. Mumtaz IM, Hoyer BF, Panne D, Moser K, Winter O, Cheng QY, Yoshida T, Burmester GR, Radbruch A, Manz RA, Hiepe F. Bone marrow of NZB/W mice is the major site for plasma cells resistant to dexamethasone and cyclophosphamide: implications for the treatment of autoimmunity. Journal of autoimmunity. 2012; 39:180–188. [PubMed: 22727274]
42. Huang H, Benoist C, Mathis D. Rituximab specifically depletes short-lived autoreactive plasma cells in a mouse model of inflammatory arthritis. Proceedings of the National Academy of Sciences of the United States of America. 2010; 107:4658–4663. [PubMed: 20176942]
43. O'Connor BP, Raman VS, Erickson LD, Cook WJ, Weaver LK, Ahonen C, Lin LL, Mantchev GT, Bram RJ, Noelle RJ. BCMA is essential for the survival of long-lived bone marrow plasma cells. The Journal of experimental medicine. 2004; 199:91–98. [PubMed: 14707116]
44. Liu Z, Davidson A. BAFF and selection of autoreactive B cells. Trends in immunology. 2011; 32:388–394. [PubMed: 21752714]
45. Jacob CO, Guo S, Jacob N, Pawar RD, Putterman C, Quinn WJ 3rd, Cancro MP, Migone TS, Stohl W. Dispensability of APRIL to the development of systemic lupus erythematosus in NZM 2328 mice. Arthritis Rheum. 2012; 64:1610–1619. [PubMed: 22127792]
46. Ramanujam M, Bethunaickan R, Huang W, Tao H, Madaio MP, Davidson A. Selective blockade of BAFF for the prevention and treatment of systemic lupus erythematosus nephritis in NZM2410 mice. Arthritis Rheum. 2010; 62:1457–1468. [PubMed: 20131293]
47. Ramanujam M, Wang X, Huang W, Liu Z, Schiffer L, Tao H, Frank D, Rice J, Diamond B, Yu KO, Porcelli S, Davidson A. Similarities and differences between selective and nonselective BAFF blockade in murine SLE. J Clin Invest. 2006; 116:724–734. [PubMed: 16485042]
48. Bethunaickan R, Berthier CC, Ramanujam M, Sahu R, Zhang W, Sun Y, Bottinger EP, Ivashkiv L, Kretzler M, Davidson A. A unique hybrid renal mononuclear phagocyte activation phenotype in murine systemic lupus erythematosus nephritis. J Immunol. 2011; 186:4994–5003. [PubMed: 21411733]
49. Mahevas M, Patin P, Huetz F, Descatoire M, Cagnard N, Bole-Feysot C, Le Gallou S, Khellaf M, Fain O, Boutboul D, Galicier L, Ebbo M, Lambotte O, Hamidou M, Bierling P, Godeau B, Michel M, Weill JC, Reynaud CA. B cell depletion in immune thrombocytopenia reveals splenic long-lived plasma cells. J Clin Invest. 2013; 123:432–442. [PubMed: 23241960]

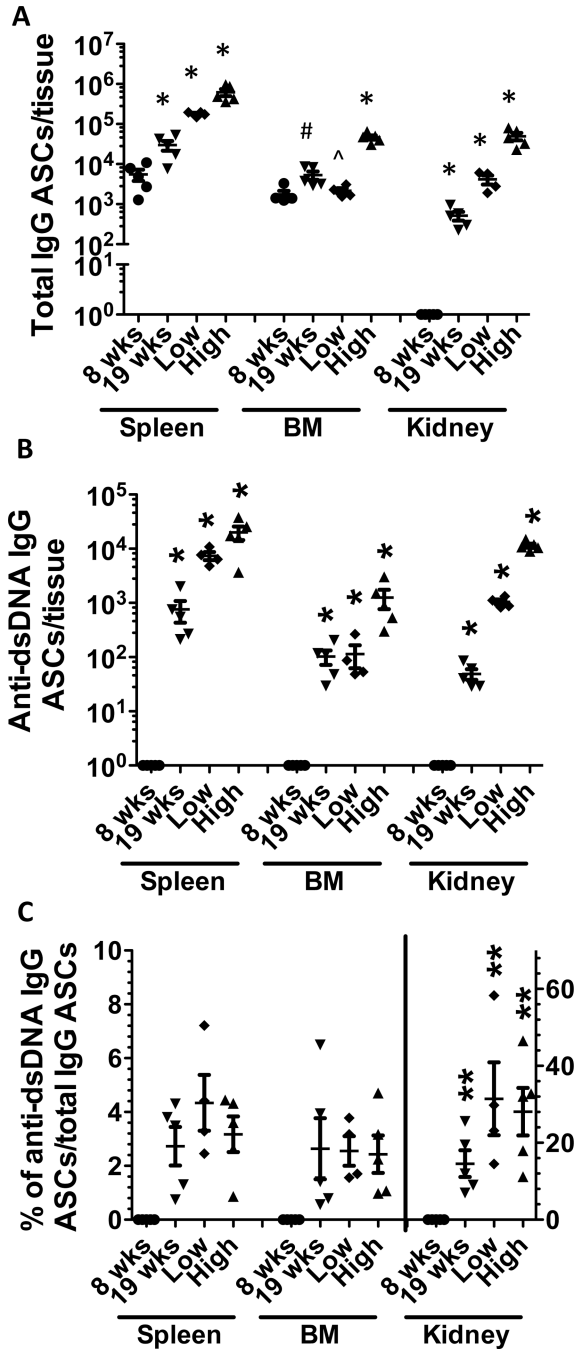

Figure 1. Total IgG and anti-dsDNA IgG ASCs accumulate with age and are highly enriched in the kidney in lupus prone mice

39 week NZB/W F1 female mice with high titer of dsDNA antibody (High) (n=5, >5-fold higher compared with that in 24 week C57BL/6 mice) were compared to that with low titer of dsDNA antibody (Low) (n=4, <3-fold higher compared with that in 24 week C57BL/6 mice). To determine the kinetics of ASC development, 8 week (n=5) and 19 week (n=5) NZB/W F1 female mice were used. Total cells from spleen, bone marrow (BM) and kidney were harvested and ELISpot assay was performed as described in “materials and methods”. Horizontal bar represent mean (long) and SEM (short). A. total IgG ASCs in spleen, BM, and kidney. B. anti-dsDNA IgG ASCs from spleen, BM and kidney. Anti-dsDNA IgG ASCs

were undetectable in 8 week NZB/W F1 female mice. C. the ratio of anti-dsDNA IgG ASCs/total IgG ASCs in spleen, BM, and kidney, respectively. Left scale for spleen and BM, right scale for kidney. Significant *p* values ($p<0.05$) (unpaired *t-test* as follows:
*significantly different from the other groups
^significantly different from high
#significantly different from high and 8 wk
**significantly different from corresponding group in spleen and BM

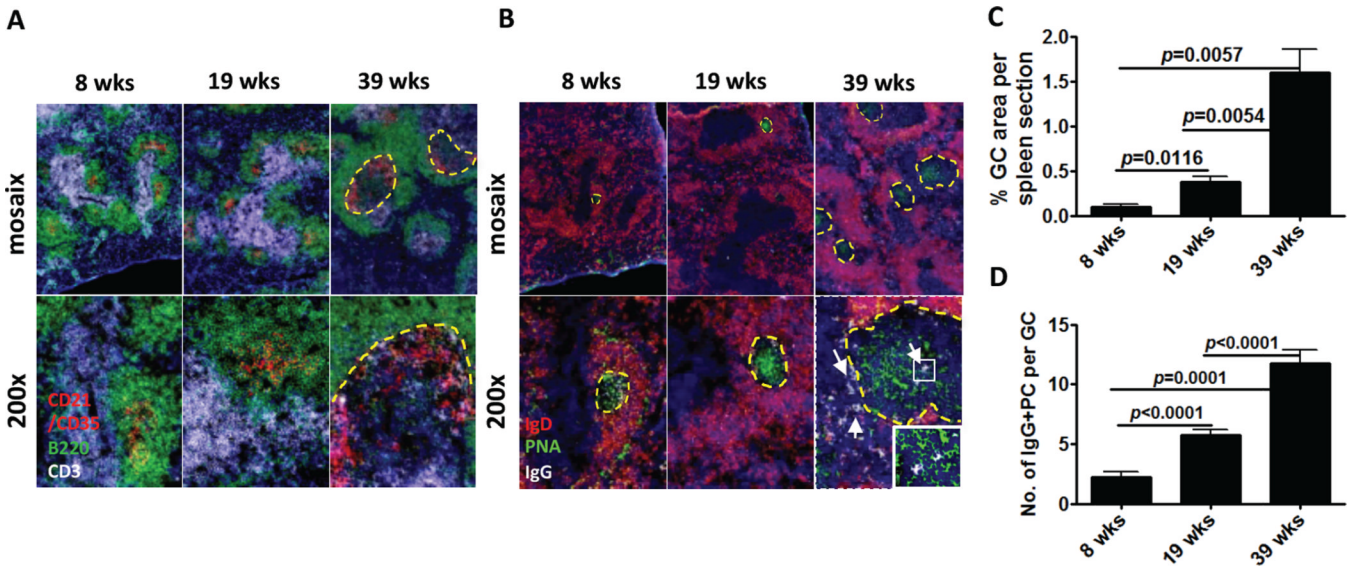

Figure 2. Kinetics of germinal center formation and plasma cell generation in murine lupus

A. Representative pictures from spleens (n=5) of each group are shown. 4 μm spleen frozen sections were probed with antibodies against CD21-CD35 (red), B220 (green) and CD3 (white) to reveal T cell spatial distribution and FDC networks. B. Antibodies against IgD (red), peanut agglutinin (green) and IgG (white) were used to detect bona fide GC and isotype-switched PC, arrow indicates isotype-switched PC. The mosaix figures in the top rows are a compilation of 16 200X images. GC is outlined with yellow dashed line. White arrows point to isotype-switched IgG+ cells. Square area is enlarged and put on left bottom. Representative data from two experiments with similar results are shown. C. GC area was measured in blinded fashion by IPLab 4.0 software. Bars show mean±SEM. *p* value is calculated with unpaired *t-test*. Average GC size and number were also significantly higher as mice aged (size: p=0.005 39 wk vs. 8 wk and p=0.0001 39 wk vs. 19 wk; number: p=0.006 39 wk vs. 8 wk and p=0.03 19 wk vs. 8 wk). n=3 8 wk, n=4 19 wk, n=5 39 wk mice. D. IgG+ plasma cells in GCs were measured in blinded fashion. Bars show mean ±SEM. *p* value is calculated with unpaired *t-test*.

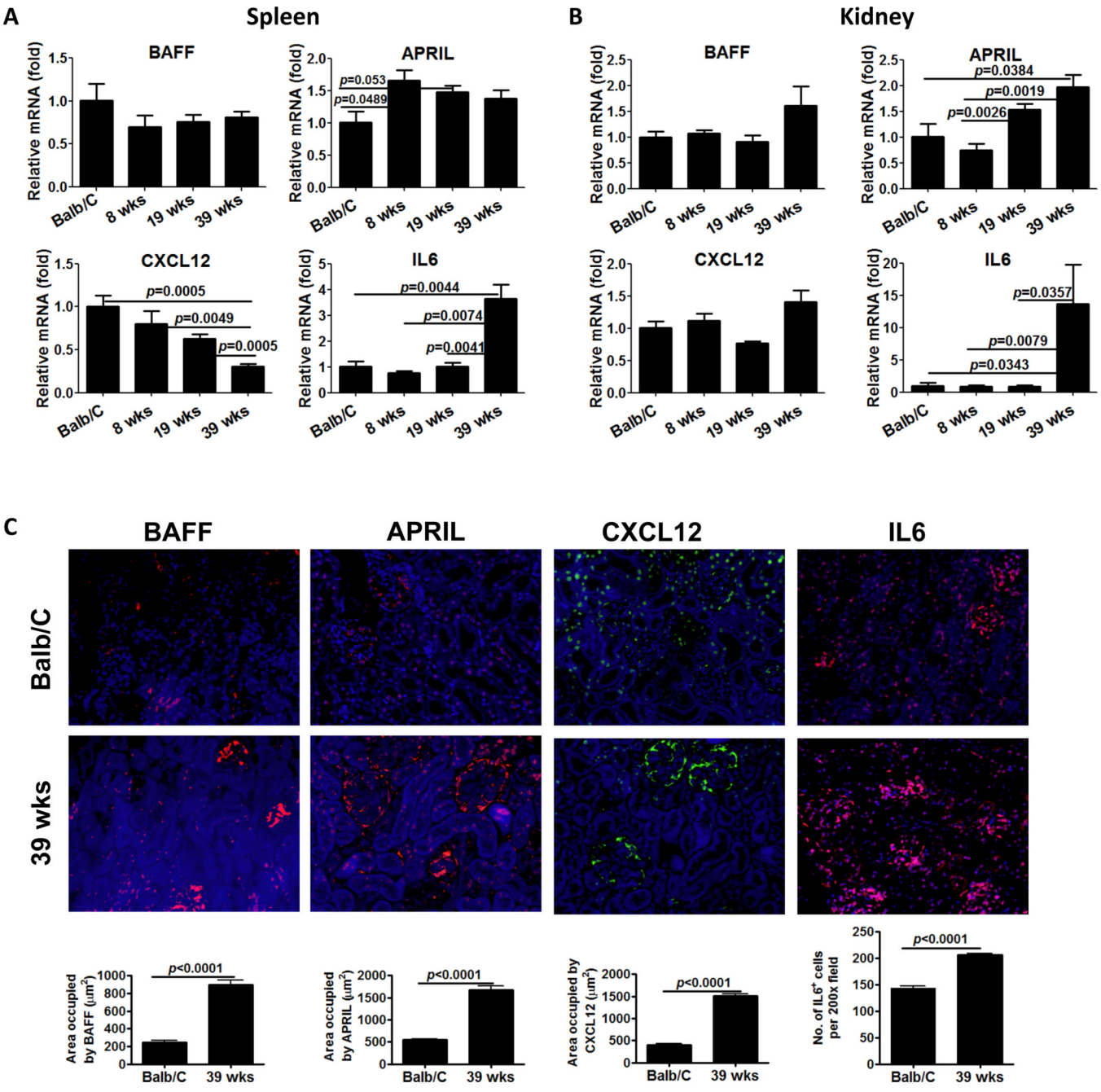

Figure 3. Changes in plasma cell survival and chemotactic factors in spleen and kidney

Total RNA was isolated from spleens (A) and kidney (B) from Balb/C control mice and NZB/W mice at the indicated age. cDNA was prepared with superscript II and random primers and concentration adjusted to 10 ng/ul. 50 ng of cDNA were used for quantitative PCR reactions using specific probes for BAFF, APRIL, CXCL12 and IL6. Levels of expression for each gene were first normalized to GAPDH and then compared to the levels of expression in Balb/C mice, according to the ΔΔCT method. Representative data from two experiments with similar results is shown. N=3–5 mice per group. Bars show mean±SEM. *p* values are calculated by Mann-Whitney *test.* C. Increase in protein expression of PC survival factors in the kidney in NZB/W mice. 4 μm frozen kidney sections were probed

with antibodies against BAFF (red), APRIL (red), CXCR12 (green) and IL6 (red). Representative pictures from kidney of each group (n=5) are shown. Quantitation of BAFF, APRIL, CXCL12 and IL6 expression was performed by morphometric analysis. Bars show mean±SEM. *p* values are calculated by unpaired *t- test.*

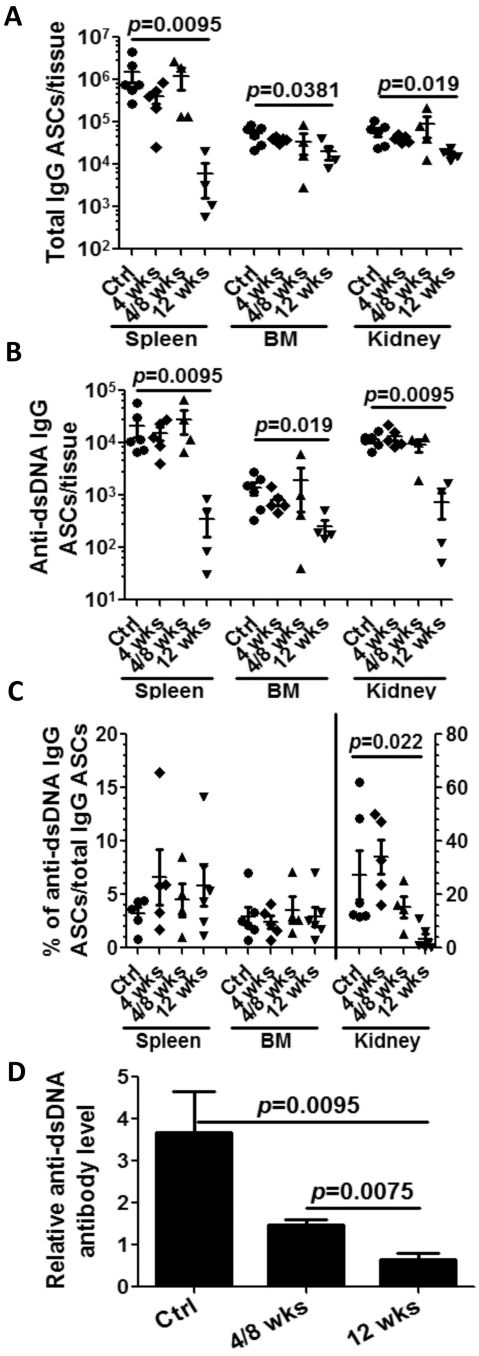

Figure 4. Long-term anti-mCD20 treatment significantly reduces antibody-secreting cells

24–28 week NZB/NZWF1 female mice with high titer anti-dsDNA antibodies were dosed weekly with anti-mCD20 antibody or control IgG (n=6, Ctrl). One group was treated 4 times weekly and sacrificed one week later after last treatment (n=5, 4 wks). One group was treated weekly×4 (n=4) and sacrificed 8 weeks later (4/8 wks). Another group was treated weekly×12 (n=4) and sacrificed 1 week after the last treatment (12 wks). Cells from spleen, bone marrow (BM) and kidney were collected and total IgG and dsDNA IgG ASCs were determined by ELISpot. Solid circle for control mice (treated for 12 wk with control IgG), solid diamond for 4 week treated mice; solid up-triangle for the mice 4/8 week mice; solid down-triangle for 12 week treated mice. Bars represent mean±SEM. *p* values were

calculated by Mann-Whitney *test*. A. total IgG ASCs from spleen, BM and kidney. Significant reduction of total IgG ASCs is observed after 12 week B cell depletion with anti-mCD20 antibody compared with untreated control mice. B. anti-dsDNA IgG ASCs from spleen, BM and kidney. Significant reduction of anti-dsDNA IgG ASCs is observed after 12 week B cell depletion with anti-mCD20 antibody compared with untreated control mice. C. the percentage of anti-dsDNA IgG ASCs/total IgG ASCs in spleen (left scale), BM (left scale) and kidney (right scale), respectively. Significant reduction of dsDNA/IgG ratio is observed after anti-mCD20 antibody treatment. D. The antibody in plasma was measured before treatment (baseline) and at endpoint, and the change relative to baseline calculated. After 12 week B cell depletion, anti-dsDNA antibody level is significantly decreased (control vs. 12 wk p value=0.0095; control vs. 4/8 wk p value NS).

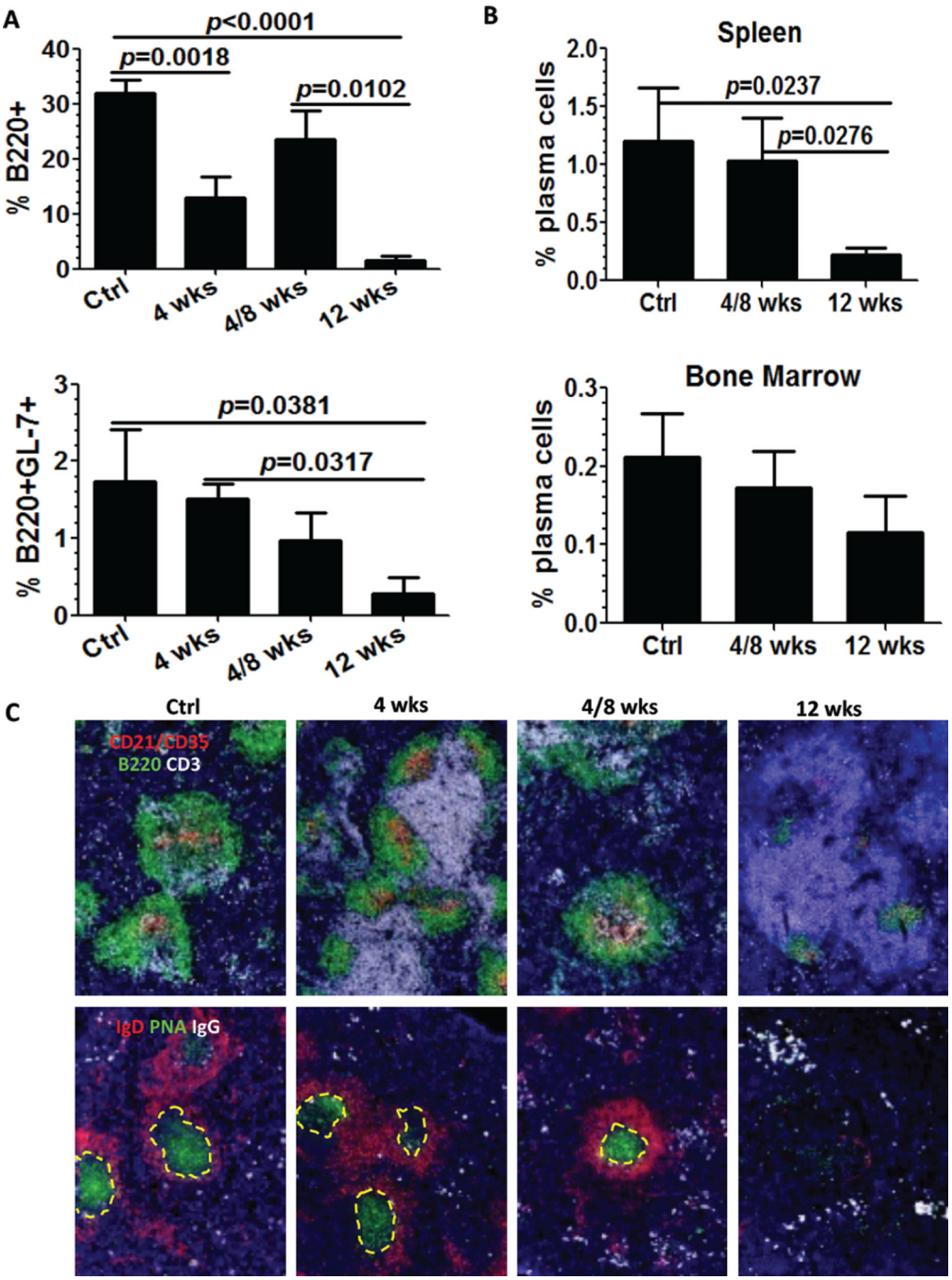

Figure 5. Long-term B cell depletion decreases plasma cell generation by dramatically reducing B cells and GCs in the spleen

As described above, four groups including control mice treated with control IgG (Ctrl) (n=6), mice treated with anti-mCD20 antibody for 4 weeks (4 wks) (n=8), mice with 8 weeks reconstitution after 4 weeks treatment with anti-mCD20 antibody (4/8 wks) (n=6), and mice treated with anti-mCD20 antibody for 12 weeks (n=4) were sacrificed. Tissue and lymphocytes were collected and analyzed by flow cytometry and immunohistochemistry. A. Percentage of residual B cells after BCD via flow cytometry expression of B220 (upper) and GL-7 (lower) in lymphocytes in spleen. B. Percentage of residual plasma cells in total cells after treatment with anti-mCD20 antibody. Plasma cells were enumerated by flow cytometry

as CD138+k light chain+ cells. Bars show mean±SEM. C. Changes in the splenic architecture associated to long-term CD20 depletion. 4 μm spleen frozen sections were stained with antibodies to detect follicular dendritic cells (CD21-CD35, red), B cells (B220, green) and T cells (CD3, white). Germinal centers and plasma cells were visualized with antibodies against IgD (red), peanut agglutinin (green) and IgG (white). GCs are outlined with dashed yellow lines. Representative of n=5 mice per group. The average number of IgG^+ cells counted in 5–10 randomly selected 200x fields significantly decreased after 12 wks BCD therapy (p=0.026).

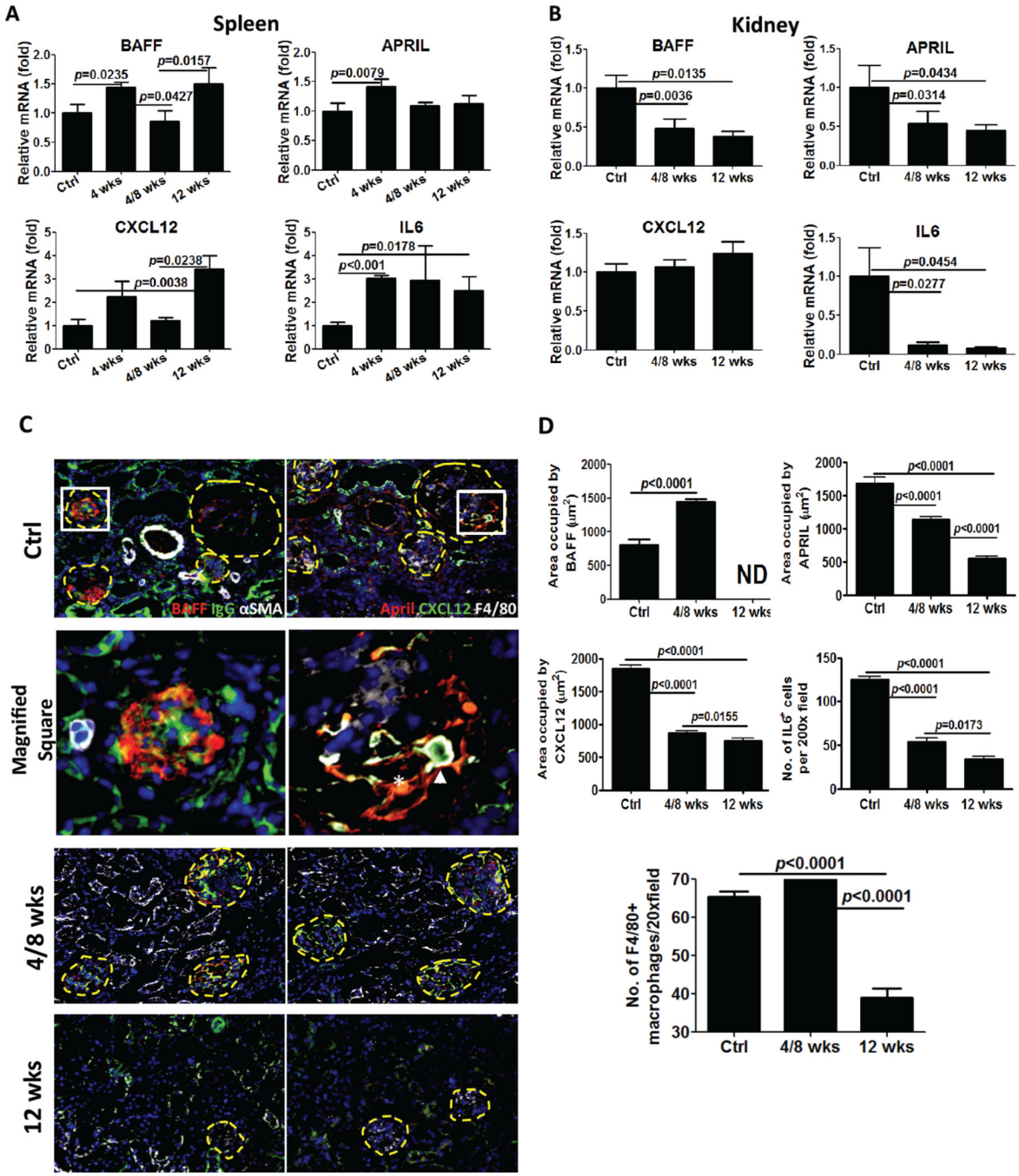

Figure 6. Long-term anti-CD20 B cell depletion alters plasma cell survival in the kidney

Total RNA was isolated from spleens (A) and kidney (B) from control group (n=8 spleen, n=12 kidney), mice treated fro 4 weeks (n=5 only spleen), 4/8 week mice (n=5 spleen and n=6 kidney), and mice treated for 12 weeks (n=4 spleen and kidney). qPCR was performed as described in Figure 3 and the Methods. Levels of expression for each gene were first normalized to GAPDH and then compared to the levels of expression in the control group, according to the ΔΔCT method. Representative data from two experiments with similar results is shown. C. Decrease in PC survival factor expression in the kidney after long-term CD20 depletion. 4 μm kidney frozen sections were stained with antibodies to detect BAFF (red), APRIL (red), IgG (green), CXCL12 (green) and IL6 (data not shown). Macrophages

were visualized with antibodies against F4/80 (white). α-SMA (white) was used for detecting myoepithelial cells. Glomeruli are outlined with dashed yellow lines. The square area stained with BAFF/IgG/α-SMA is magnified and shown on left middle. The square area stained with APRIL/CXCR12/F4/80 is magnified and shown on right middle. The arrow highlights a CXCL12 expressing macrophage. The asterisk highlights a stromal cell co-expressing APRIL and CXCL12. Representative of n=5 mice per group, quantitated in D. D. Quantitation of F4/80+ macrophages, BAFF, APRIL, CXCR12 and IL6 expression was performed by morphometric analysis and reveals a significant decrease after BCD (ND=non detected). Bars show mean±SEM. *p* values are calculated by unpaired *t- test.*